

Quantum Chessboards in Deuterium Wavepackets

C R Calvert¹, T Birkeland², R B King¹, I D Williams¹, J F McCann¹ - *19 March 2022*

1. School of Mathematics and Physics, Queen's University Belfast, BT7 1NN, UK

2. Department of Mathematics, University of Bergen, N-5007, Bergen, Norway

E-mail: tore.birkeland@math.uib.no

Abstract. We present a novel scheme for quantum manipulation in ultrafast diatomic molecules. A pump mechanism is used to create a coherent superposition of the D_2^+ vibrations. A short, intense, control pulse is applied, after a fractional coherence time, to create selective interferences. A 'chessboard' pattern of states can be realised in which the set of even/odd numbered vibrational states can be annihilated. A technique is proposed for experimental realization and observation of this effect using 5fs pulses of $\lambda = 790\text{nm}$ radiation, with intermediate intensities ($\sim 5 \times 10^{13} \text{ W cm}^{-2}$). We identify a new algorithm for vibrational control that is feasible with current experimental technology.

PACS numbers: 32.80.Qk, 42.50.Hz, 42.50.Md

Keywords: intense laser, molecule, coherent control

1. Introduction

The ability to effect quantum control at the molecular level has many potential applications, such as control of reaction dynamics [1], selective electron localisation [2], and applications in quantum information processing [3]. In order to characterize control mechanisms and afford useful comparison between experiment and theory, the diatomic hydrogen molecule (and its ion, H_2^+) is often used as a test-bed in such investigations. These systems are extremely useful because of their simple electronic structure. The heavier isotopes of hydrogen, such as deuterium and deuterium hydride are equally accessible for quantum simulations and execute slower nuclear motion, thus deuterium (D_2) has become the preferred target for experimental studies with femtosecond pulses.

In recent years, ultrashort laser pulses have been used to initiate, image [4, 5] and control [6, 7] the ultrafast dissociation of D_2^+ , with the localisation of the remaining bound electron also manipulated [2]. However, such control of fundamental molecular motion has not been limited to dissociation dynamics, and progress has been made on studies of bound wavepacket motion, with control mediated by interactions occurring on timescales shorter than the motion itself. For example, coherent rotational motion in

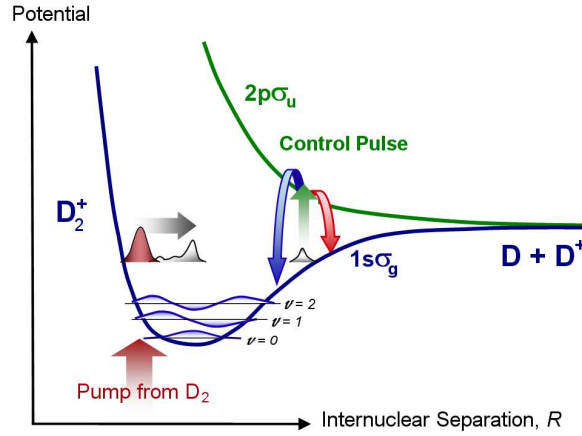


Figure 1. Schematic of intense field vibrational control of D_2^+ (not to scale). An ultrashort pump pulse tunnel-ionizes a D_2 target to initiate a coherent superposition of D_2^+ $1s\sigma_g$ vibrations. The vibrations de-phase and the wavepacket disperses (silver arrow). The application of a secondary, control pulse initiates Raman transitions via the virtual $2p\sigma_u$ levels. The subsequent mode mixing can lead to vibrational cooling (blue arrow) or heating (red arrow).

molecules can now be induced and controlled [8, 9] in fast diatomic systems due to the availability of intense-field pulses on sub-rotational (typically picosecond) timescales, where mapping of rapidly rotating (hydrogenic) diatomics has been achieved [10, 11].

Several proposals for coherent control of vibration in the deuterium molecular ion have been put forward, with similar underlying principles [3, 12, 13]. Firstly, an ultrashort ‘pump pulse’, in this case a Ti:Sapphire laser, is used to induce tunnel-ionization of the neutral target. In this process, the transition time (tunneling time) is fast relative to the optical period, and is essentially instantaneous with respect to the relaxation time for vibration/rotation. That is, the transition is vertical, to a good approximation, and the Franck-Condon approximation applies. Taking, $t = 0$, as the moment of creation of the molecular ion state, the subsequent vibration is given by the eigenfunction expansion:

$$|\Psi(t)\rangle = \sum_n a_n |n\rangle \exp(-iE_n t/\hbar) \quad , \quad (1)$$

where, $\{|n\rangle\}$ denotes the set of vibrational eigenstates (discrete and continuous) of the molecular ion, and $\{E_n\}$ the corresponding energies. In this case only a few per cent of the wavepacket escapes to the continuum, with the bulk contained within the 28 discrete states.

The anharmonicity of the potential means that the components dephase within a few vibration cycles [14]. The wavepacket reforms whenever the phases of the components in (1) match. This quantum ‘revival’ (at $t \sim 550$ fs) was recently measured [15, 16] and well-reproduced by simulations [16, 17]. These experiments also demonstrated that the slow rotation of the molecule was found to play a minor role [16]

in the process.

Suppose that, after a time τ , a secondary (control) pulse is used to alter the wavepacket. It has been shown that an infrared pulse produces an AC Stark-effect that distorts the potential well (adiabatically) and hence modifies the wavepacket motion[12]. Dissociation occurs, but also a relative enhancement of lower vibrational populations was noted. While the adiabatic picture provides a useful physical interpretation, it does not fully explain the redistribution process.

In an alternative view, a Raman-type scheme has been proposed [3, 13] where portions of the wavepacket may be transferred between the $1s\sigma_g$ (bound) and $2p\sigma_u$ (dissociative) potential, as seen in Figure 1. In recent simulations, high-intensity pulses ($I \geq 10^{14}$ W cm $^{-2}$) have been used to enforce vibrational squeezing or ‘quenching’ into a specific state [13] or to create a coherent 2 (or 3) state wavepacket [3]. These studies were conducted with short delay times ($\tau < 100$ fs), where the first-order ($n - n' = \pm 1$) vibrational beat components are dephasing.

In this article, we show that intermediate intensity ($I \sim 5 \times 10^{13}$ W cm $^{-2}$), few-cycle (5 fs) control pulses have important applications for coherent manipulation. We find a fascinating and hitherto unseen ‘chessboard’ pattern in the redistribution. In a different outcome to previous quenching/cooling studies, it is possible to selectively enhance almost *exclusively even* or *exclusively odd* numbered vibrational states. It is found that the mechanism of this process relies on constructive/destructive interference. This effect can be exploited at the fractional revival time to create strong-contrast interference patterns.

2. Simulations of Vibrational Control

Coherent wavepacket motion in D_2^+ can be initiated by ultrafast intense-field tunnel-ionization of a D_2 target on sub-vibrational timescales [14]. This has recently been demonstrated with pump pulse durations of 7 – 15 fs [15, 17]. Coherence is lost for pump pulses much longer than the vibrational period (~ 25 fs) [14, 16]. The initial D_2 target can be assumed to reside in the ground vibrational state of the $X^1\Sigma_g$ potential. The ionization event will project this vibration function onto the manifold of vibrational states of the ion. This is the usual ‘vertical’ (Franck-Condon) transition. Although this is a simplified picture [13, 18] in recent experiments [16, 17] with pump pulses ($\lambda = 790$ nm) of duration 10 – 15 fs, with intensities $I = 5 - 8 \times 10^{14}$ W cm $^{-2}$ experimental evidence seems to support the assumption. In fact, the Franck-Condon principle is not an essential requirement for the control process that we propose, since other initial conditions can be treated in a similar manner.

At intermediate intensities with infrared frequencies, such as those we consider, higher-lying states are inaccessible. In our model we solve the time-dependent equation for evolution on the two lowest potential curves ($1s\sigma_g$ and $2p\sigma_u$). Thus the configuration space can be partitioned into g and u components. Then the Hamiltonian,

H , can be partitioned into vibration, electronic motion, and laser interaction as follows:

$$H = T_R + H_e + V \quad . \quad (2)$$

This has the matrix representation:

$$H = \begin{pmatrix} T_R & 0 \\ 0 & T_R \end{pmatrix} + \begin{pmatrix} \varepsilon_g(R) & 0 \\ 0 & \varepsilon_u(R) \end{pmatrix} + \begin{pmatrix} 0 & F(t)d(R) \\ F(t)d(R) & 0 \end{pmatrix} \quad , \quad (3)$$

where T_R is the vibrational kinetic energy operator, $\varepsilon_g(R)$ and $\varepsilon_u(R)$ are the potential energy curves for the $1s\sigma_g$ and $2p\sigma_u$ electronic states respectively, and $d(R)$ is the dipole moment between these states [19]. The external electric field $F(t)$ is created by a Ti:Sapphire laser with $\lambda = 790\text{nm}$, modulated by a Gaussian profile centred at $t = \tau$ (the delay time), with full-width-half-maximum of W (the duration), that is:

$$F(t) = F_0 \cos(\omega(t - \tau)) \exp\{-2 \ln 2(t - \tau)^2/W^2\} \quad . \quad (4)$$

The (cycle-average) intensity, I , of the pulse is related to the electric field amplitude, F_0 , by the formula, $I = \frac{1}{2}\epsilon_0 c F_0^2$. The evolution of the equations is computed by a symmetric, split-step algorithm [20]:

$$\begin{aligned} |\psi(t + \Delta t)\rangle &= \exp(-iT_R \Delta t/2) \exp(-iH_e \Delta t/2) \exp(-iV(t) \Delta t) \\ &\times \exp(-iH_e \Delta t/2) \exp(-iT_R \Delta t/2) |\psi(t)\rangle + O(\Delta t^2) \quad . \end{aligned} \quad (5)$$

The error in this expression arises partly from the splitting (factorisation) and from assuming the Hamiltonian changes slowly over the time step (time-ordering error). In practice, the time-step Δt is chosen sufficiently small so that, $\Delta t(\partial H/\partial t) \ll H$.

The splitting and the use of a uniform grid means the highly-efficient fast Fourier transform [21] can be employed. The electronic coupling term V is diagonal in the radial dimension, and a diagonalization of the 2×2 submatrix gives an efficient scheme for propagation:

$$\begin{aligned} &\exp \left[-i\Delta t \begin{pmatrix} 0 & F(t)d(R) \\ F(t)d(R) & 0 \end{pmatrix} \right] = \\ &\frac{1}{2} \begin{pmatrix} \mathbb{1} & \mathbb{1} \\ -\mathbb{1} & \mathbb{1} \end{pmatrix} \begin{pmatrix} \exp(-iF(t)d(R)\Delta t) & 0 \\ 0 & \exp(iF(t)d(R)\Delta t) \end{pmatrix} \begin{pmatrix} \mathbb{1} & -\mathbb{1} \\ \mathbb{1} & \mathbb{1} \end{pmatrix} \quad , \end{aligned} \quad (6)$$

where $\mathbb{1}$ is the unit matrix. The vibrational populations are projections of the g -state wavepacket on the manifold, $\{|n\rangle\}$, while the dissociation yield will be defined by the population in the u state along with the g -state continuum.

3. The Chessboard

The vibrational populations, following the application of a short control pulse ($W = 5$ fs), with $I = 5 \times 10^{13} \text{ W cm}^{-2}$, were calculated for a range of delay times $0 \leq \tau \leq 600\text{fs}$. The results are presented in Figure 2. The colour density in Figure 2(a) represents the final population of a vibrational level with respect to the control pulse delay. The

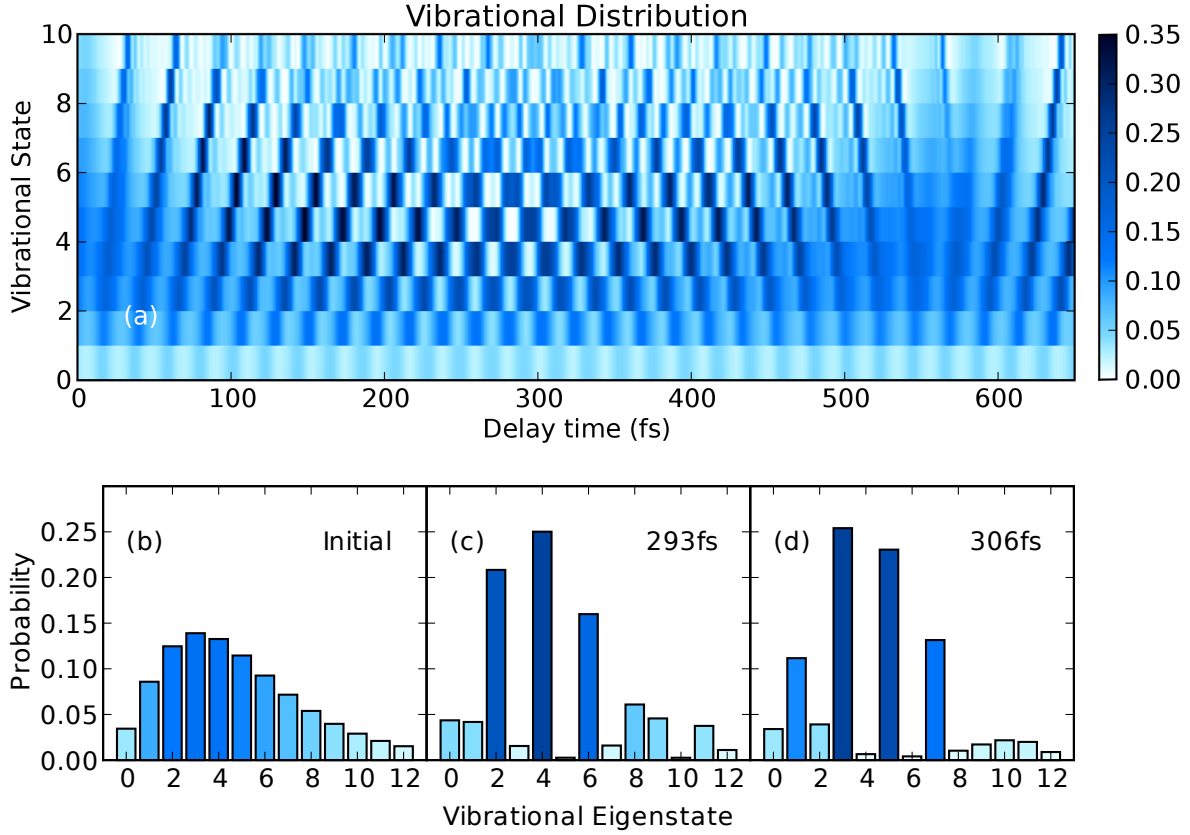


Figure 2. Vibrational distributions following a $\lambda = 790\text{nm}$, $W = 5\text{ fs}$, $I = 5 \times 10^{13}\text{ W cm}^{-2}$ control pulse, as a function of delay time τ . (a) The colour density represents the relative population of each level. (b) Initial probability distribution. For short delay times, $\tau < 100\text{ fs}$, and near the revival, $\tau \sim 550\text{fs}$, the control pulse redistributes broadly with only slight enhancement in any single level. In contrast, the ‘chessboard’ pattern (centred around the half-revival $\tau \sim 300\text{ fs}$) shows an interference pattern in which even or odd numbered states are annihilated. For $\tau = 293\text{ fs}$ and $\tau = 306\text{ fs}$, cuts through the colourmap are shown in (c) and (d).

distributions resulting from $\tau = 293\text{ fs}$ and $\tau = 306\text{ fs}$ are extracted from Figure 2(a) and displayed as the bar charts 2(c) and 2(d), respectively. The initial probability distribution is shown in Figure 2(b).

In previous studies, the modulations in population had been attributed to the classical vibrational period of each level [13]. Our conclusion is different, and we will show that they are regulated by an interference process.

For short delays ($\tau < 50\text{ fs}$) the anharmonic correction is small, and dephasing is not significant. Under such conditions, the control pulse spreads the population evenly with only slight enhancements/deficits. In the region $\tau \sim 100\text{ fs}$, enhancement is concentrated in a specific level (e.g. $n = 4$ at $\tau = 100\text{ fs}$). These effects are repeated around the wavepacket revival ($\sim 550\text{ fs}$), where the wavepacket begins to reform. Higher-intensity control pulses can be used to optimize both these cases of state-selective control [3, 13]

and drive population towards one or more specific levels.

The most striking feature of Figure 2(a) is the alternating light and dark squares, suggestive of a ‘chessboard’ pattern, centred around $\tau \sim 300$ fs. At this half-revival time, the even and odd vibrational subsets will be in phase with each other. This partial coherence can be exploited to produce interference effects. In this case we find that a chessboard pattern can be created. The effect is illustrated in Figure 2(c), where the non-negligible populations are *exclusively* in *even* numbered states. Likewise for $\tau = 306$ fs, this effect occurs for *odd* numbered states, with $n = 1, 3, 5, 7$, strongly favoured.

The effect can be understood by the destructive/constructive interference nearest-neighbour modes. Suppose we consider the effect of the pulse on isolated states $n = 3, 4, 5$, separately. In Figure 3 the final amplitudes and phases on the manifold are illustrated by bar charts and clocks. These clocks indicate the phase shift of the state with respect to the unperturbed state; that is all clocks will remain at 12 o’clock in the absence of any perturbation.

In each case, starting with a single vibrational state, the final probability distribution is independent of τ . We also note a selection rule favouring neighbouring levels. For example, at the half-revival time $\tau = 293$ fs, the contribution to $|4\rangle$ from all three initial states have roughly the same phase, i.e. they interfere constructively. In contrast, with $\tau = 306$ fs, the contributions from $|3\rangle$ and $|5\rangle$ are almost opposite to the contribution from $|4\rangle$, giving a destructive interference. For the final population in $|5\rangle$, the situation is opposite, yielding destructive and constructive interference for $\tau = 293$ fs and 306 fs respectively. This pattern is repeated so that even numbered states get enhanced and odd numbered states get quenched for $\tau = 293$ fs, and opposite for $\tau = 306$ fs giving rise to the chessboard effect seen in Figure 2.

4. Model

A simple mathematical model of the interference can be obtained from perturbation theory. As a preliminary comment, the hierarchy of timescales in this system are worth noting, from the fast electronic motion to the medium speed optical field, through to the comparatively ‘slow’ vibrational motion. The ‘electronic time’ is of the order of the dissociation energy of the molecule, with an associated angular frequency: $\sim 25 \times 10^{15} \text{rad s}^{-1} \approx 0.6 \text{a.u.}$, while the optical cycle time is $\omega_{\text{opt}} \sim 2.4 \times 10^{15} \text{rad s}^{-1} \approx 0.06 \text{a.u.}$, and finally the vibration time $\omega_e \sim 0.3 \times 10^{15} \text{rad s}^{-1} \approx 0.007 \text{a.u.}$ Consequently the pulse interaction is sudden compared to the vibrational timescale, but adiabatic in the context of the electronic motion.

The effect of a laser pulse after a delay τ can now be considered. A simple mathematical model can be constructed where the modulated sinusoidal signal of the laser pulse is considered as a sequence of alternating square waveforms. The expansion

$$|\psi(t)\rangle = \sum_{\gamma, n} a_{\gamma, n}(t) e^{-iE_{\gamma, n}t} |\gamma, n\rangle \quad (7)$$

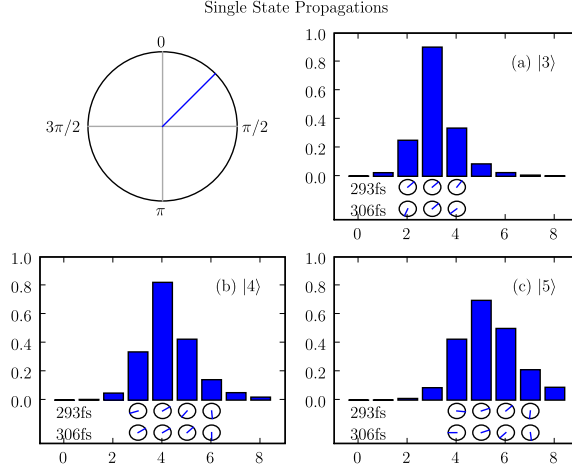


Figure 3. Vibrational transfer starting from (a) $n = 3$, (b) $n = 4$ and (c) $n = 5$ by a 5fs, $\lambda = 790$ nm, $I = 5 \times 10^{13}$ W cm $^{-2}$ control pulse. The bar charts present the probabilities, $|a_n|^2$, while the clocks display the phase of the coefficients, a_n , after the pulse, for $\tau = 293$ fs (1) and $\tau = 306$ fs (2). The distributions are concentrated around the initial state, while the initial state is phase-advanced. This illustrates that a coherent sum of the final distributions will depend strongly on τ .

can be proposed as the solution to

$$i\hbar \frac{\partial}{\partial t} |\psi(t)\rangle = H(t) |\psi(t)\rangle \quad (8)$$

where $\gamma \in \{g, u\}$ is the electronic state with corresponding vibration state (bound and/or dissociative) n . Equation (8) can be written as a set of integral equations ($t \geq t_0$):

$$a_{\gamma,n}(t) = a_{\gamma,n}(t_0) - i \sum_{\gamma',n'} \int_{t_0}^t dt' a_{\gamma',n'}(t') V_{\gamma,n;\gamma',n'}(t') \exp[i\Delta_{\gamma,n;\gamma',n'} t'] \quad (9)$$

where $\Delta_{\gamma,n;\gamma',n'} = E_{\gamma,n} - E_{\gamma',n'}$ and the coupling potential V is expanded in the basis set in equation (7), such that

$$V_{\gamma,n;\gamma',n'}(t') = \langle \gamma, n | V | \gamma', n' \rangle = F(t) d_{\gamma',n';\gamma,n} \quad (10)$$

The photon energy (~ 0.06 a.u. in this case) is below the single-photon dissociation threshold for all states of the g potential with $n < 8$, and for laser intensities lower than 10^{14} W cm $^{-2}$, the upper electronic level u acts merely as a virtual state. Since, for a homonuclear molecule such as D $_2$, we have $d_{\gamma,n;\gamma',n'} = 0$ when $\gamma = \gamma'$, for all n, n' , this implies that the leading-order coupling is quadratic.

The expansion coefficients of (7), can then be calculated to second-order accuracy:

$$a_{\gamma,n}(\tau + W) = a_{\gamma,n}(0) + (-i)^2 \sum_{\gamma',n',\gamma'',n''} \int_{\tau}^{\tau+W} dt' \exp[i\Delta_{\gamma,n;\gamma',n'} t'] V_{\gamma,n;\gamma',n'}(t') \quad (11)$$

$$\times \int_{\tau}^{t'} dt'' \exp[i\Delta_{\gamma',n';\gamma'',n''} t''] V_{\gamma',n';\gamma'',n''}(t'') a_{\gamma'',n''}(0) \quad (12)$$

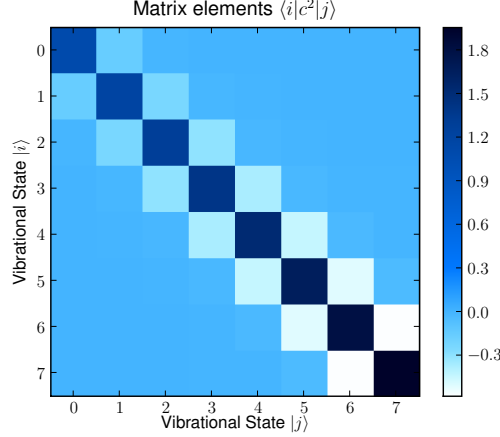


Figure 4. Second-order coupling strength between vibration eigenstates during the laser pulse d_{ij}^2 . (a) shows coupling strength between adjacent levels, while (b) shows coupling strength between all levels for $n < 8$. Notice the rapid decrease in coupling strength as $|i - j|$ grows leading to an approximate selection rule $i - j \in \{-1, 0, 1\}$ for weak fields. Also notice that the coupling strength increases with vibrational levels, giving a rise to a slight heating, i.e. propensity towards higher vibrational levels.

For simplicity, consider the pulse to be applied impulsively after a delay τ , for a duration W' (corresponding to half an optical cycle), with amplitude F_0 . A further simplification can now be made in the summation over the intermediate states. The 'closure approximation' replaces the spectrum of intermediate energies by a constant, $E_{\gamma',n'} = \bar{E}$, representative of the dominant (resonant) channels. In the spirit of the approximation, we choose \bar{E} as the threshold of dissociation in the u state. Then taking this as the reference point for the zero of energy, we simply set $\bar{E} = 0$. The closure (completeness) relation can then be applied so that:

$$\sum_{\gamma',n'} d_{\gamma,n;\gamma',n'} d_{\gamma',n';\gamma'',n''} = d_{\gamma,n;\gamma'',n''}^2 \quad (13)$$

The index γ may now be dropped for convenience, since all states except the ground-state ($\gamma = g$) have been eliminated. Thus a simple expression for the expansion coefficients is obtained:

$$a_n(\tau + W') = a_n(0) - \sum_{n''} a_n''(0) d_{n,n''}^2 F_0^2 \int_{\tau}^{\tau+W'} dt' e^{iE_n t'} \int_{\tau}^{t'} dt'' e^{-iE_{n''} t''} \quad (14)$$

and this may be evaluated without further approximation.

As seen in Figure 4, the matrix element $d_{n,n''}^2$ provides an approximate selection rule: $n' = n, n \pm 1$, so that the expression can be reduced even further. Moreover, since $E_n W' \gg 1$, then the solution can be expressed in the simple form:

$$a_n(\tau + W') \approx a_n(0) (1 - i\kappa_{nn}) - i\kappa_{n,n-1} a_{n-1}(0) e^{i(E_n - E_{n-1})\tau} - i\kappa_{n,n+1} a_{n+1}(0) e^{i(E_n - E_{n+1})\tau} \quad (15)$$

where

$$\kappa_{n,n'} = \left(\frac{F_0^2 d_{n,n'}^2}{E_{n'}} \right) \left(\frac{\exp[i(E_n - E_{n'})W'] - 1}{i(E_n - E_{n'})} \right) \quad (16)$$

In the case of a very short impulse, corresponding to a half-cycle, $(E_n - E_{n-1})W' \ll 1$, and:

$$\kappa_{n,n'} \approx \left(\frac{F_0^2 W'}{E_{n'}} \right) d_{n,n'}^2 \quad (17)$$

The term $\kappa_{n,n}$ simply reflects the change in phase due to the quadratic Stark effect. Since this is a second-order effect, the sign of F_0 has no consequence, and $\kappa_{n,n} < 0$, and hence there is a phase advance. This is illustrated in Figure 3 where the parent state is phase shifted forward, with the excited state $n = 5$ more advanced than the state $n = 3$, in agreement with this expression. We note that, in this model, $\kappa_{n,n'}$ is not sensitive to sign of F_0 , that is, to the carrier envelope phase. Thus a sequence of alternating half-cycles creates the same effect as a full-wave rectified pulse.

Consider the effect of one half-cycle. The equations above have the simple explanation that $a_n(\tau + W')$ is created by an interference pattern with its immediate neighbours. This pattern can be regular if the terms on the right hand side are coherent. In order to create strong destructive interference, the terms $(\kappa_{n,n-1}a_{n-1}(0) + \kappa_{n,n+1}a_{n+1}(0))$ must be approximately the same size as the remaining term $a_n(0)(1 - \kappa_{n,n})$ for $n \in 2 \dots 6$. This gives an optimal value of F_0 and W' . Next, the phases of the two interference terms must be equal, which implies the condition (for all n):

$$(E_n - E_{n-1})\tau = -(E_{n+1} - E_n)\tau \quad , \quad \text{mod}(2\pi) \quad . \quad (18)$$

A rough estimate of this condition on τ , can be made by the anharmonic expansion, $E_n \approx -D_e + \hbar\omega_e(n + \frac{1}{2}) - \hbar\omega_e x_e(n + \frac{1}{2})^2$, where D_e is the dissociation energy. This is satisfied during the fractional revival around $\tau \approx \pi/(2\omega_e x_e) \sim 280$ fs. Finally, these terms must be out of phase with a_n to create destructive interference. The Stark effect (15) creates a phase shift, $-\kappa_{n,n}$, for the state n . Thus in order to get destructive interference, the requirement is then

$$\kappa_{n,n} = (E_n - E_{n-1})\tau + \pi/2 \quad , \quad \text{mod}(2\pi) \quad . \quad (19)$$

If destructive interference occurs for even n , then according to equation (18), constructive interference will be observed for odd n . Furthermore, if destructive interference is observed for a state at $\tau = \tau_0$, constructive interference will be observed for $\tau = \tau_0 + \pi/\omega_e \approx \tau_0 + 11$ fs. This is a qualitative explanation, and is limited by the crudeness of the closure approximation. Further, the assumptions we make for the pulse are unduly simple. Nevertheless, it appears that this simple model explains the main features that we observe in the numerical simulations.

5. Experimental Technique for Observing the Chessboard

Having simulated the chessboard pattern and explained the underlying mechanism, attention can be turned to techniques for experimental observation of this fascinating

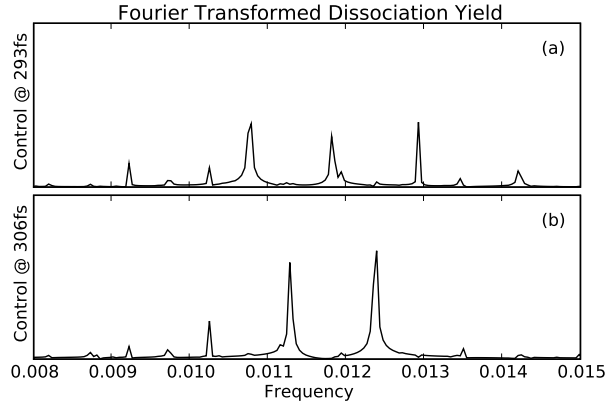


Figure 5. Spectral density for the dissociation yield correlation function. The coherent D_2^+ wavepacket is controlled by a 5 fs, $\lambda = 790\text{nm}$, $I = 5 \times 10^{13} \text{ W cm}^{-2}$ pulse at $\tau = 293 \text{ fs}$ and $\tau = 306 \text{ fs}$ for plots (a) and (b) respectively. The probe pulse is, $\lambda = 790\text{nm}$, $I = 4 \times 10^{14} \text{ W cm}^{-2}$, duration 12 fs. Fourier analysis of the dissociation signal returns the vibrational beats $\omega_{n,n'}$ present in the wavepacket motion in each case. The probe delay time ranges from 310 fs to 4000 fs. A shorter range of times, 310 fs to 1000 fs for example, gives similar features. In this case the peaks are broadened but still well resolved.

effect. In previous pump-probe studies, vibrational wavepacket motion has been imaged by using a probe pulse to enforce photodissociation or Coulomb explosion of the vibrating molecule. Spectral analysis of the fragmentation yield can return a measure of both the temporal and spatial nature of the wavepacket motion, which can even lead to full characterisation of the molecular motion [22]. In particular the beat frequencies that dictate the motion of the probability density, can be extracted from the photodissociation signal.

Thus it may be possible to conduct a pump-control-probe experiment where a new coherent vibrational distribution (created at a specific control pulse delay time) may be monitored by recording the total dissociation yield as a function of probe delay time (τ') and subsequently applying spectral analysis. Such a scheme has been simulated here by fixing the control pulse at a desired τ value and then including a secondary (probe) pulse at a variable delay time, τ' . The probe pulse (5 fs duration, $I = 3 \times 10^{14} \text{ W cm}^{-2}$) was applied and the dissociation yield was deduced by subtracting the remaining bound population from the initial norm of the wavepacket. The Fourier transform (energy spectral density) of the dissociation signal is shown in Figure 5 for respective control delay times of (a) $\tau = 293 \text{ fs}$ and (b) $\tau = 306 \text{ fs}$. The calculations represent the signal correlation over very long times (4000fs). On such timescales, rotational decoherence may be significant. However, we have performed the same analysis over a much shorter time (1000fs) and, although the features are broadened, the signatures are still clearly visible.

The individual states in vibrational distribution are not resolved in isolation but rather the peaks in Figure 5(a) correspond to the beat frequencies $\omega_{4,2}$ and $\omega_{6,4}$.

These are notably absent in Figure 5(b), where only the odd numbered eigenstate beat frequencies are observed, in keeping with the expected vibrational distributions (from Figure 2). The amplitude of the beat $\omega_{n,n'}$ in the wavepacket motion is given by $|a_n a_{n'}|$, however the photodissociation signal is stronger for highly excited vibrations, the Fourier transform technique will not measure the absolute population values, $|a_n a_{n'}|$. Rather the spectrum will verify which states contain any significant population and therefore provide a useful tool for experimentally identifying the preferential creation of either *even* or *odd* numbered states. It should be noted however that periods of the $\omega_{n,n+2}$ beats are typically 10 – 12 fs and thus for any possible experimental observations of this nature, it is imperative that pulses of around 5 fs are used.

In principle, this technique using the photodissociation signal appears to be a useful pathway for identifying the main components of the wavepacket and with state-of-the-art pulses now widely available for durations $W < 10$ fs, this should be achievable in the laboratory in the not too distant future. Indeed, with continuing advances in intense-field laser-pulse experiments, such an even (or odd) state wavepacket (evolving with ~ 12 fs oscillations) may even be well characterized by using a high-intensity probe pulse and a very recently proposed ‘time-series analysis’ of the Coulomb explosion signal [23], where full reconstruction of the wavepacket has been proposed as a future extension.

6. Conclusion

In this article, the application of an intermediate intensity ($I \sim 5 \times 10^{13}$ W cm⁻²) few-cycle ($W = 5$ fs) control pulse to a coherent vibrational wavepacket in D₂⁺ has been investigated. The redistribution of vibrational levels proceeds by a Raman transfer between near-neighbour levels. This creates interferences such that it is possible to produce strong-contrast fringes of the even/odd numbered vibrational levels.

The ‘chessboard’ pattern that emerges around $\tau \sim 275 - 300$ fs provides a pathway for creating almost *exclusively even* or *exclusively odd* numbered vibrational distributions in a coherent wavepacket. The subsequent propagation of such a created wavepacket may be probed via photodissociation and here it has been shown that spectral analysis of the dissociation data may serve to identify the populated states. This provides a pathway for using currently available ultrashort laser pulse technology to investigate this ‘chessboard’ effect.

Acknowledgments

C R Calvert and R B King wish to acknowledge funding from Department of Employment and Learning (NI).

References

- [1] Mokhtari A, Cong P, Herek J L and Zewail A H 1990 *Nature* **348** 225

- [2] M F Kling, Ch Siedschlag, A J Verhoef, J I Kahn, M Schultze, Y Ni, Th Uphues, M Uiberacker, M Drescher, F Krausz, M J J Vrakking 2006 *Science* **312** 246-248
- [3] Murphy D S, McKenna J, Calvert C R, Williams I D and McCann J F 2007 *New J. Phys* **9** 260
- [4] Trump C, Rottke H and Sandner W 1999 *Phys. Rev. A*. **59** 2858
- [5] Ergler Th, Rudenko A, Feuerstein B, Zrost K, Schröter C D, Moshhammer R and Ullrich J 2005 *Phys. Rev. Lett.* **95** 093001
- [6] Murphy DS *et al* 2007 *J. Phys. B*. **40** S359
- [7] Niikura H, Villeneuve D M and Corkum P B 2006 *Phys. Rev. A*. **73** 021402
- [8] Lee K F, Shapiro E A, Villeneuve D M and Corkum P B 2006
- [9] Fleischer S, Averbukh I Sh and Prior Y 2008 *J. Phys. B*. **41** 074018
- [10] Lee K F, Légare F, Villeneuve D M and Corkum P B 2006 *J. Phys. B*. **39** 4081
- [11] Bryan W A, English E M L, McKenna J, Wood J, Calvert C R, Torres R, Turcu I C E, Collier J L, Williams I D and Newell W R 2007 *Phys. Rev. A*. **76** 023414
- [12] Niikura H, Villeneuve D M and Corkum P B 2004 *Phys. Rev. Lett.* **92** 133002
- [13] Niederhausen T and Thumm U 2008 *Phys. Rev. A*. **77** 013407
- [14] Feuerstein B and Thumm U 2003 *Phys. Rev. A* **67** 063408
- [15] Ergler Th, Rudenko A, Feuerstein B, Zrost K, Schröter C D, Moshhammer R and Ullrich J 2006 *Phys. Rev. Lett.* **97** 193001
- [16] Bryan W A *et al* 2007 *Phys. Rev. A* **76** 053402
- [17] McKenna J *et al* 2007 *J. Mod. Opt.* **54** 7 1127
- [18] Urbain X, Fabre B, Staicu-Casagrande E M, de Ruelle N, Andrianarijaona V M, Jureta J, Posthumus J H, Saenz A, Baldit E and Cornaggia C 2004 *Phys. Rev. Lett.* **92** 163004
- [19] Bates D R 1951 *J Chem Physics* **19** 1122
- [20] Hermann M R, Fleck J A 1988. *Phys. Rev. A* **38** 6000.
- [21] Frigo M, Johnson S G 2005 *Proceedings of the IEEE* **93(2)** 216
- [22] Feuerstein B, Ergler Th, Rudenko A, Zrost K, Schrter C D, Moshhammer C D, Ullrich J, Niederhausen T and Thumm U 2007 *Phys. Rev. Lett.* **99** 153002
- [23] Thumm U, Niederhausen T and Feuerstein B 2008 *Phys. Rev. A*. **77** 063401